

# Investigation of bioactive nanofiber-based scaffolds for cultivated meat.

Ana Elisa Antunes dos Santos<sup>1</sup>, Tiago Cotta<sup>2</sup>, João Paulo Ferreira Santos<sup>2</sup>, Juliana Sofia Fonseca Camargos<sup>2</sup>, Ana Carolina Correia do Carmo<sup>2</sup>, Erika Gabriele Alves Alcântara<sup>3</sup>, Claudia Fleck<sup>3</sup>, Aline Gonçalves Lio Copola<sup>1</sup>, Júlia Meireles Nogueira<sup>1</sup>, Gerluza Aparecida Borges Silva<sup>1</sup>, Erika Cristina Jorge<sup>1</sup>, Luciana de Oliveira Andrade<sup>1</sup>, and Roberta Viana Ferreira<sup>2</sup>

<sup>1</sup>Universidade Federal de Minas Gerais

<sup>2</sup>Centro Federal de Educacao Tecnologica de Minas Gerais

<sup>3</sup>Technische Universitat Berlin

August 16, 2022

## Abstract

Synthetic polymers scaffolds often need to be coated with extracellular matrix (ECM) proteins to improve cell adhesion. For cultivated meat applications, coating should be avoided since it is necessary to eliminate expensive and animal-derived components. As cellulose acetate nanofibers is a low-cost cellulose-derived material, that induces cell adhesion and proliferation, we investigated its use associated with a bioactive annatto extract, a food-dye and potential meat preservative, as scaffolds for cultivated meat. Here, the bioactive electrospun nanofibers were evaluated through morphological, mechanical and biological characterizations. The results revealed that the scaffolds were porous with no specific alignment and average fiber diameter of  $420\pm 212$  nm. Molecular analyzes revealed that in contrast to cellulose acetate scaffold, annatto-loaded cellulose acetate scaffold favor a proliferative state of C2C12 mouse skeletal myoblasts. SEM microscopy images suggests that the nanofiber substrates can sustain long-term culture of the cells, up to 28 days. These results suggest that the combination of cellulose acetate fibers loaded with annatto extract may be an interesting economical alternative for support long-term muscle cells culture with potential application as a scaffold for cultivated meat and muscle tissue engineering.

**Title:** Investigation of bioactive nanofiber-based scaffolds for cultivated meat.

**Authors:** , Ana Elisa Antunes dos Santos<sup>§1</sup>, Tiago Cotta<sup>§2</sup>, João Paulo Ferreira Santos<sup>2</sup>, Juliana Sofia Fonseca Camargos<sup>2</sup>, Ana Carolina Correia do Carmo<sup>2</sup>, Erika Gabriele Alves Alcântara<sup>3</sup>, Claudia Fleck<sup>3</sup>, Aline Gonçalves Lio Copola<sup>1</sup>, Júlia Meireles Nogueira<sup>1</sup>, Gerluza Aparecida Borges Silva<sup>1</sup>, Erika Cristina Jorge<sup>1</sup>, Luciana de Oliveira Andrade<sup>1</sup>, Roberta Viana Ferreira<sup>\*2</sup>.

## Affiliation:

<sup>1</sup> Department of Morphology, Institute of Biological Science, Federal University of Minas Gerais, Belo Horizonte, Minas Gerais, 31270-901, Brazil.

<sup>2</sup> Department of Materials Engineering, Federal Center for Technological Education of Minas Gerais (CEFET-MG), Av. Amazonas 5253, 30.421-169, Belo Horizonte, MG, Brazil.

<sup>3</sup> Technische Universität Berlin, Chair of Materials Science & Engineering, Straße des 17. Juni 135 – Sekr. EB13, 10623 Berlin, Germany.

§ These authors contributed equally.

\*Corresponding Author: Roberta Viana Ferreira; e-mail address:

*robertavia@gmail.com*

Tel.: +41-797495840

## Abstract

Synthetic polymers scaffolds often need to be coated with extracellular matrix (ECM) proteins to improve cell adhesion. For cultivated meat applications, coating should be avoided since it is necessary to eliminate expensive and animal-derived components. As cellulose acetate nanofibers is a low-cost cellulose-derived material, that induces cell adhesion and proliferation, we investigated its use associated with a bioactive annatto extract, a food-dye and potential meat preservative, as scaffolds for cultivated meat. Here, the bioactive electrospun nanofibers were evaluated through morphological, mechanical and biological characterizations. The results revealed that the scaffolds were porous with no specific alignment with an average fiber diameter of  $420\pm 212$  nm. Molecular analyzes revealed that in contrast to cellulose acetate scaffold, annatto-loaded cellulose acetate scaffold favor a proliferative state of C2C12 mouse skeletal myoblasts. SEM microscopy images suggests that the nanofiber substrates can sustain long-term culture of the cells, up to 28 days. These results suggest that the combination of cellulose acetate fibers loaded with annatto extract may be an interesting economical alternative for support long-term muscle cells culture with potential application as a scaffold for cultivated meat and muscle tissue engineering.

**Keywords:** cultivated meat, cellulose acetate, annatto, nanofiber, scaffold, muscle tissue engineering

## 1. Introduction

Cultivated meat is an emerging technology that aims to obtain meat products through animal muscle tissue growth in a controlled environment, applying tissue engineering techniques [1]. The interest in cultivated meat (also known as in vitro meat, clean meat, cultured meat, cell-based meat or lab-grown meat) is motivated by several factors: potential increase in future demand for animal protein, concerns about the environmental impact of current meat production methods and occupation of land to raise animals, greenhouse gas emissions resulting from meat production and animal welfare, which has become an important issue for many consumers [2,3].

Tissue engineering techniques are used to provide a suitable and complex environment for cells or tissue to be grown on scaffolds, biomaterials capable of mimicking the extracellular matrix of the animals, which can support the development and growth of complex skeletal muscle tissues [4,5]. One stage in meat cultivation is controlled growth and maturation of myoblasts in scaffolds [6,7]. Scaffolds are a key component for cell agriculture, serving as an integrated support network in which cells expand and differentiate in ways that depend on anchorage [10]. A fundamental approach for cultivated meat is to extend the replicative capacity of skeletal muscle precursor cells for expansion on an industrial scale [8,9]. In this sense, scaffolds for cultivated meat must support proliferation and long-term stable culture of muscle cells under conditions that mimic the animal's body. Therefore, additional research is needed to improve the design of scaffolds appropriate for myoblast cultivation in order to obtain muscle fibers.

Electrospun nanofiber scaffolds present an interesting alternative for muscle cells cultivation because they can better simulate typical muscle fibrous architecture. The nanoscale structure mimics the extracellular matrix morphology and induce great cellular attachment due to nanofiber high aspect ratio, scaffold porosity and surface-to-volume ratio [11]. Previous studies have demonstrated the importance of the nanoscale structure and its anisotropy in synthetic polymers for the development of 3D matrices [18,19]. Besides this, the nanofibers contribute to rapid diffusion of oxygen and nutrients, as well as cell infiltration. In addition, nanofiber scaffolds have the ability to induce cell alignment along the fibers that may induce muscle fiber maturation [12]. Although various nanofiber scaffolds have been developed for biomedical applications, few investigations have been done for applications in cultivated meat.

Cellulose-based biomaterials offer some important advantages over conventional synthetic materials and show

great scientific promise [13]. Several studies have demonstrated that the hydrophilic hydroxyl moieties of the cellulose and specialized cellulose binding domains provides sites that favor adhesion and proliferation [14,15]. Cellulose acetate (CA) is a modified natural polymer that has good solubility and can be easily controlled morphologically [16,17]. CA nanofibers are very interesting in cultivated meat applications because, in addition to being a biocompatible material, their fabrication by the electrospinning process is relatively easy [14]. Besides, contrary to scaffolds composed of plant-based materials, they do not need to be coated with ECM proteins or chemical modification to improve cell adhesion [13, 27]. Santos et al. (2021) demonstrated that it is possible to grow fibroblasts on cellulose acetate nanofibers without the need for coating [26]. Thus, the application of cellulose acetate nanofibers in a cultured meat production process may be a more economical option compared to other synthetic polymers. Nevertheless, studies with cellulose acetate nanofibers for applications in tissue engineering and cultured meat are still scarce.

Another important point in food production is preservation, which nowadays is focused on the use of natural products [20]. Recently, essential oils extracted from plants have received a lot of attention due to their meat protection properties. Antimicrobial properties of plant essential oils are derived from some main bioactive components such as phenolic acids, terpenes, aldehydes, and flavonoids that are present in essential oils [21]. Various mechanisms such as changing the fatty acid profile and structure of cell membranes and increasing the cell permeability as well as affecting membrane proteins and inhibition of functional properties of the cell wall are effective in antimicrobial activity of essential oils. [22].

Annatto is the fruit of the annatto (*Bixa orellana* L.) native to South America. Annatto seeds are considered antibiotics of medicinal character, acting as an anti-inflammatory for bruises and wounds, also having use in the cure of bronchitis and external burns. In addition, annatto has a long history of use in the food industry as a natural dye [23,24,25]. Our research group, produced scaffolds from cellulose acetate nanofibers loaded with annatto extract and demonstrated that the scaffold maintained the viability of mouse fibroblasts after 48 h of culture in addition to the cells attached, spread and colonized the nanofiber scaffold [26].

Here, we investigated morphological, mechanical and biological features of a bioactive nanofiber scaffolds previously developed by our research group, to evaluate their potential for application in cultivated meat. We found that cellulose acetate nanofibers loaded with annatto extract favored cell adhesion and improved cell viability and long-term cell proliferation.

## 2. Materials and methods

### 2.1 Materials

Annatto extract (containing the main components bixin, norbixin, and carotenoids) was purchased from Amazonia Forest Trading (Manaus, Brazil). Cellulose acetate (CA) in powder form, with  $M_n \sim 30,000$  g/mol, density of 1.3g/ml, and 40% degree of substitution was purchased from Sigma-Aldrich (São Paulo). The solvent used to obtain annatto extract was ethanol, and for electrospinning acetone and N,N-dimethylformamide (DMF), all from Labsynth (Diadema, Brazil). For biological assays, Dulbecco's Modified Eagle medium (DMEM), fetal bovine serum (FBS), penicillin-streptomycin-amphotericin B solution (anti-anti), and 3-(4,5-dimethylthiazolyl-2)-2,5-diphenyltetrazolium bromide (MTT) were all purchased from Gibco-Invitrogen (São Paulo, Brazil).

### 2.2 Preparation of nanofibers

Cellulose acetate solution was prepared using 9 ml acetone, 3 ml dimethylformamide, 1.44 g cellulose acetate, and 1% wt annatto extract, as previously described [26]. The solution was mixed with an IKA HS 7 magnetic stirrer for 2 h at RT. When utilized, annatto extract was added after mixing all the other components to mitigate degradation.

The cellulose acetate nanofibers (CA) and cellulose acetate nanofibers with annatto extract (CA@A) were obtained by electrospinning, as previously described [26]. Briefly, the cellulose acetate and cellulose acetate loaded with annatto extract were dissolved in acetone-dimethylformamide (3:1 v/v) to obtain 12 wt% (w/v) solution. The polymer solution was fed into a 10 mL standard syringe attached to a 0.8 mm diameter steel

needle and spun on an NB-EN1 (NanoBond, China) electrospinning device with electric voltage of 16 kV, 14 cm working distance, collector rotation at 400 rpm, and solution gravity-fed at room temperature.

### *Physicochemical characterization*

UV-vis spectroscopy of annatto extract was performed in a Perkin Elmer Lambda 1050 spectrometer (Waltham, USA) with wavelength range of 250–800 nm and scanning speed of 267 nm/min. The annatto extract used in this analysis was diluted in acetone 1:50 (v/v), and measured immediately after the extract was prepared. Samples were evaluated by Fourier transform infrared spectroscopy (FTIR) using a Shimadzu IRPrestige-21 device in the range between 4000 and 400  $\text{cm}^{-1}$ .

Morphology was evaluated with a Phenom XL (Phenom-World, Eindhoven, Netherlands) scanning electron microscope (SEM) using medium vacuum (60 Pa) and auto focus on an accelerating voltage of 5 kV. Samples were sputtered with gold for 20 minutes using a sputter coater (Cressington 108 model; Cressington Scientific Instruments, Watford, England). Average fiber diameter and size distribution were obtained with ImageJ software based on the SEM images. From three SEM images of each sample, 200 fibers were randomly selected and their diameter measured manually using the Line tool.

Surface wettability of the nanofibers was measured using deionized water at room temperature with a contact angle analyzer (KRÜSS model DSA-100; KRÜSS Scientific, Hamburg, Germany). Deionized water was automatically dripped onto the samples and five contact angle measurements were averaged to obtain a reliable value.

Thermogravimetric analysis (TGA) of the nanofibers was conducted with a TA Instruments Q50 device (TA Instruments, New Castle, USA), heating the samples from room temperature to 900 °C at 20 °C/min in  $\text{N}_2$  atmosphere.

### *2.4 Mechanical characterization*

Nanoscale dynamic mechanical analysis (Nano-DMA) tests were performed at room temperature using a Hysitron TI950 TriboIndenter device (Bruker Corporation, Billerica, USA) equipped with a Berkovich tip. Samples were glued to an epoxy holder to ensure stability during measurement. A grid with 100 measurement points (10 x 10) was created for oscillatory measurements to simultaneously obtain both the linear- and visco-elastic responses of the sample. Specimens were loaded with a sinusoidal force-time-function and a maximum load of 75  $\mu\text{N}$  oscillating at eight different frequencies (10, 31, 25, 115, 136, 157, 178, and 201 Hz). Loss ( $E''$ ) and storage modulus ( $E'$ ) were calculated from the measured force-displacement hysteresis loops using the software provided with the Bruker nanoindenter. The indents are approximately twice as small as the fiber diameter; we assumed that if an indent reached a pore, it would measure the fiber directly below it.

### *2.5 Cell culture*

Immortalized mouse myoblasts (C2C12) were seeded onto the nanofibers (CA and CA@A) and onto the monolayer as a control. Before cell seeding, scaffolds were sterilized using gamma irradiation. The materials were irradiated at room temperature with a standard dose of 10 kGy.  $^{60}\text{Co}$  gamma-ray source was used. Gamma irradiation sterilization was carried out at Gamma Irradiation Laboratory installed at the Nuclear Technology Development Centre (CDTN), Belo Horizonte, Brazil. Both scaffolds were equilibrated using 200  $\mu\text{l}$  of growth medium (GM) [GM: DMEM-high glucose (Gibco), supplemented with 10% bovine fetal serum (Gibco) and 1% anti-anti (Gibco)] for 24 h before cell seeding. C2C12 cells were used in the 4<sup>th</sup> and 8<sup>th</sup> passages, in triplicate. Cells were seeded at a density of  $8 \times 10^4$  cells/well in 24-well plates. After 2 h of incubation at 37°C and 5%  $\text{CO}_2$ , the volume of GM was completed to 500  $\mu\text{l}$ /well.

### *2.6 MTT assay for cell viability*

Cell viability was assessed using MTT (3-(4,5-dimethylthiazol-2-yl)-2,5-diphenyl tetrazolium bromide) (Invitrogen), according to the manufacturer's instructions.

C2C12 cells were seeded onto the scaffolds or as a monolayer at a density of  $8 \times 10^4$  cells/well in a 24-well

plate in GM. After 2 and 7 days, GM was replaced with the MTT solution, and the samples were incubated for 2 h at 37 °C and 5% CO<sub>2</sub>. Formazan crystals were then dissolved in 1 ml/well of isopropanol-acid (100 ml isopropanol:134 ul of hydrochloric acid). Next, the solution was then transferred to a 96-well plate in triplicate and absorbances were measured at 595 nm using a microplate reader (ELX800 device; BioTek, Winooski, USA).

### 2.7 Cell counting

Cells were seeded onto the scaffolds at a density of 8x10<sup>4</sup> cells/well in GM. After 24 h, supernatants were carefully collected from the scaffolds and transferred to a new tube. The well was carefully washed with PBS, which was also transferred to the same tube containing the supernatant. Tubes containing GM and PBS from each individual well were centrifuged at 1000 rpm (approximately 184 g) for 5 minutes, and each pellet was resuspended in 50 µl of fresh GM. Cells were counted using a Neubauer chamber.

### Cell morphology and actin labeling

Morphology of the cells after growth in different substrates was analyzed by scanning electron microscopy (SEM). First, the samples were fixed in 2.5% glutaraldehyde for 6-h. The samples were rinsed with distilled water and gradually dehydrated in two increasing series of ethyl alcohol (35%, 50%, 70%, 85%, 95% and 100% for 15 minutes/bath). Samples were metalized with gold and visualized using a Quanta 200 FEG SEM (FEI, Hillsboro, USA).

For actin labeling, the scaffolds or coverslips containing the cells were washed twice with PBS and then fixed in 3.7% formaldehyde for 15 minutes at RT. The samples were then washed with PBS, permeabilized in 0.1% Triton-X100 in PBS for 10 minutes at RT, washed again with PBS, and incubated with 0.2 µg/mL Alexa Fluor 546 phalloidin (Thermo Fisher) in PBS for 30 minutes at RT. Next, the cells were washed with PBS and cell nuclei were stained with DAPI (diluted to 1:1,000 in PBS) for 20 min at RT. Images were captured in a Zeiss fluorescence microscope

### 2.9 RT-qPCR

Cells were seeded onto each scaffold or cultured as a monolayer (as described above) in triplicate and cultivated for 7 days in GM only, or for 7 days in GM followed by an additional 7 days in differentiation medium (DM: high glucose DMEM supplemented with 2% horse serum [Gibco] and 1% anti-anti [Gibco]). Both GM and DM were replaced with fresh medium every two days. All cells from the triplicate were then harvested in 1 mL TriReagent (Sigma-Aldrich) and the total RNA was isolated according to the manufacturer's instructions. Next, 1 µg of each total RNA sample was converted into cDNA, following the instructions in the RevertAid H minus first strand cDNA synthesis kit (Thermo Fischer Scientific). RT-qPCR was performed using a Corbett 3000 device (Qiagen, Helden, Germany), 0.4–0.8 µM of each primer, 1 µl (diluted 1:10) of each cDNA, and 5 µl of iTaq Universal SYBR Green Supermix (Bio-Rad, Hercules, USA) in a final volume of 10 µl. Reactions were performed as follows: 50 °C for 2 min, 95 °C for 2 min, followed by 45 cycles of 94 °C for 15 sec, 60–62 °C for 15 sec, and 72 °C for 20 sec. The dissociation step was performed at the end of the amplification step to identify the specific melting temperature for each primer set.

GAPDH was used as a reference gene. Relative gene expression was determined using REST2009 software (based on the model by Pfaffl et al., 2001) [28]. *MyoD*, *MyoG* and *Myf5* were used as target genes with the following primers: for *MyoD* (GTGGCAGCGAGCACTACA and GACACAGCCGCACTCTTC), for *MyoG* (TGAGAGAGAAGGGGGAGGAG and CGGTATCATCAGCACAGGAG), and for *Myf5* (GCAAAGACCCGTGACTTCAC and GCATGTGGAAAAGTGATA). The relative gene expression for each gene was determined by comparing the levels of gene expression in cells cultivated onto scaffolds and in cells cultivated in a monolayer. REST 2009 software [28] was used to determine statistical significance.

### Statistical analysis

All quantitative data are presented as means ± standard derivations, and three repeated experiments were given. Statistical analyses were performed using Student's t-test or one-way analysis of variance followed by

Fisher’s post hoc least-significant difference test for multiple comparisons. Differences were deemed significant at  $p < 0.05$ .

### 3. Results and Discussion

#### 3.1 Physicochemical and thermal characterization

In order to confirm previous results obtained from Santos et al. (2021) [26], results of UV-vis spectroscopy analysis of annatto extract, CA nanofibers, and CA@A nanofibers are presented in Figure 1. The annatto extract spectrum revealed a strong absorption band at 410, which can be attributed to bixin and norbixin [29,30,31]; according to Calogero et al. (2015) [30], these two substances exhibit absorption bands above 400 nm due to an electronic-dipole transition oriented along the axis of the molecule. For carotenoids such as bixin and norbixin, the  $p/p^*$  transition is relevant; in this conjugated system, the p-electrons are highly delocalized and the excited state is of comparatively low energy. As a result, relatively little energy is required to cause the transition, which corresponds to absorption in the visible region and can be attributed to the peak obtained in the spectrum. No peaks attributed to other annatto compounds were observed. This result agrees with previous work demonstrating that annatto seed extraction with low polarity solvents produces highly concentrated extracts mainly comprised of cis-bixin (70–80%) along with lesser quantities of other carotenoids as trans-bixin, cis-norbixin, and trans-norbixin [30,31,32,33,34,35,36]. The UV spectrum of CA@A nanofiber samples revealed a low-intensity absorption band centered at 410 nm, confirming the presence of annatto extract.

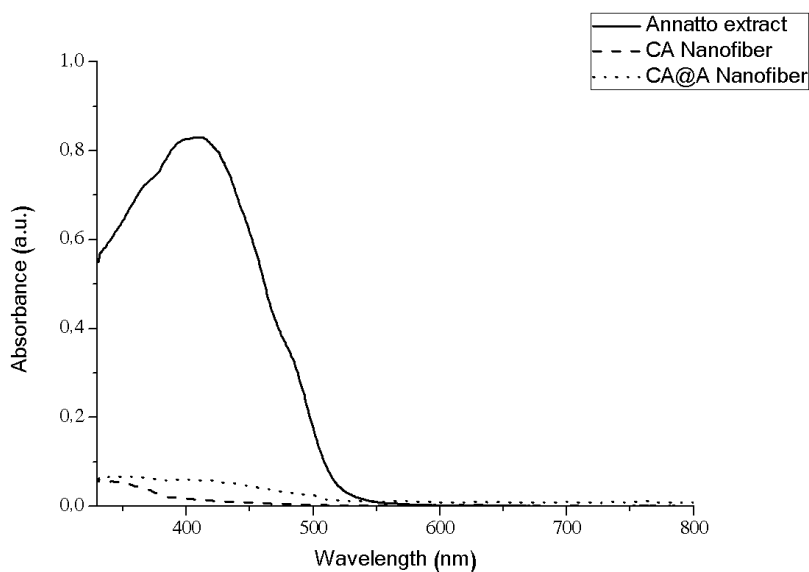


**Figure 1.** UV-vis spectra of annatto extract, cellulose acetate nanofibers (CA), and cellulose acetate nanofibers with annatto extract (CA@A).

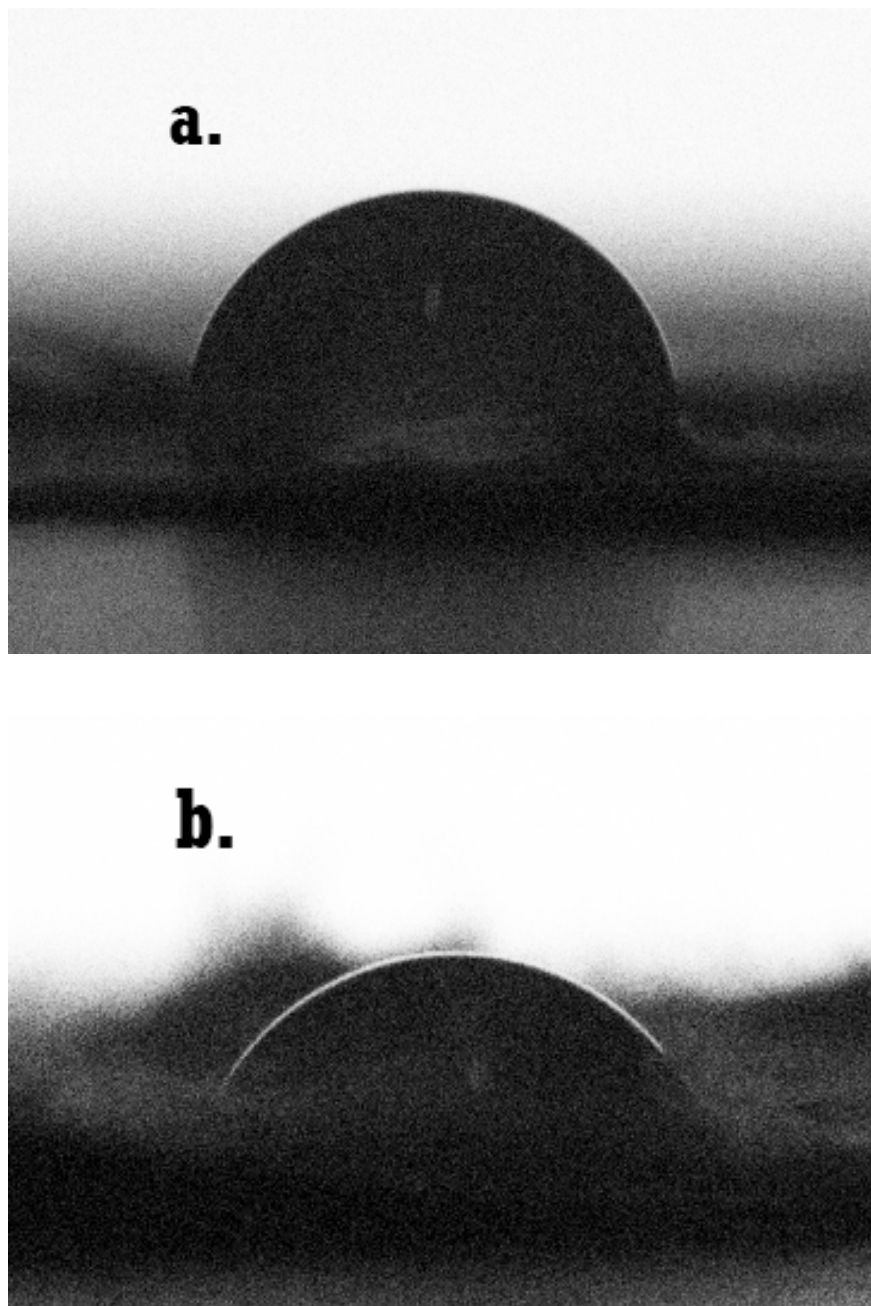


**Figure 2 .** Water contact angles of cellulose acetate nanofiber (CA) (a) and cellulose acetate nanofiber impregnated with annatto extract (CA@A) (b).

As Figure 2 shows, both nanofiber types were hydrophilic, with contact angles below  $90^\circ$ . The contact angle for the CA nanofiber was approximately  $77 \pm 3^\circ$ , while adding annatto to the CA decreased the contact angle to  $50 \pm 3$ . This effect can be attributed to the hydrophilic nature of annatto molecules such as norbixin. A more hydrophilic nanofiber surface is ideal for supporting cell attachment. According to Menzies et al. [37], the hydrophilicity of a material directly corresponds to its capacity for cell adhesion. Improved wettability (evidenced by low contact angle values in water tests) results in improved biocompatibility for the analyzed material.

### 3.2 Nanofiber morphology

Figures 3 and 4 present SEM micrographs and diameter frequency distribution (%) for CA and CA@A nanofiber scaffolds, respectively. Under SEM, both the pure and annatto-containing cellulose acetate nanofibers present smooth and relatively homogenous porous mats and exhibit porous interconnectivity, which is ideal for cell migration and scaffold colonization. Average fiber diameter was  $284 \pm 130$  nm for CA and  $420 \pm 212$  nm for CA@A.

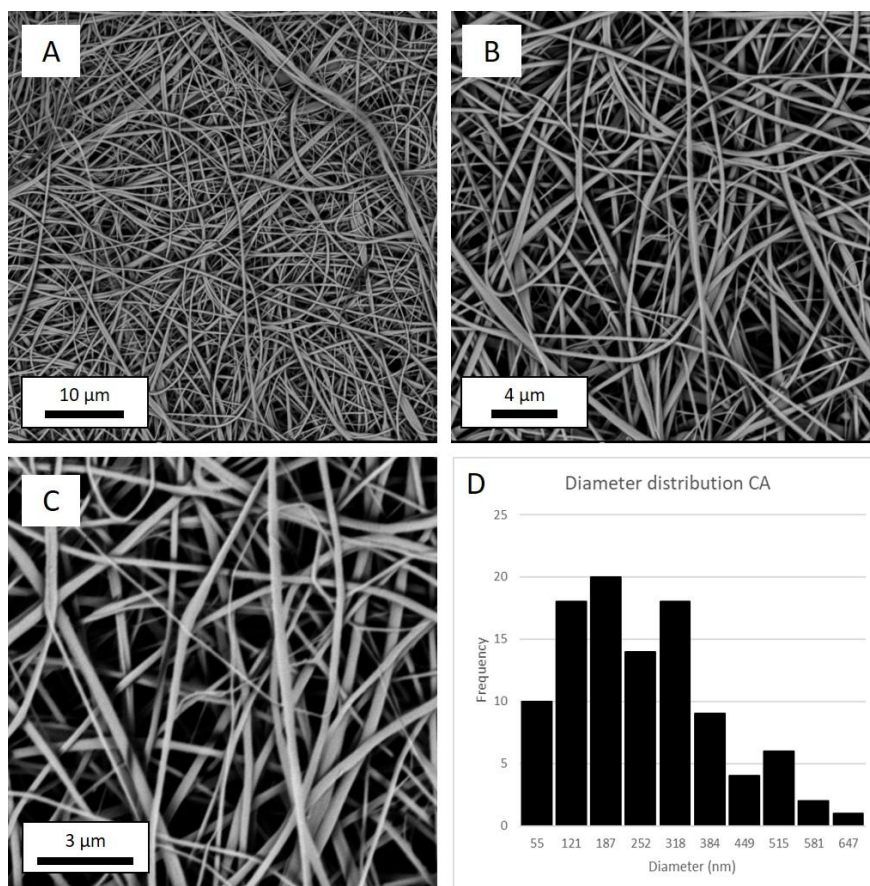


**Figure 3.** Scanning electron microscopy (SEM) images of cellulose acetate (CA) nanofibers at different magnifications (A, B, C) and diameter distribution of CA nanofibers (D).

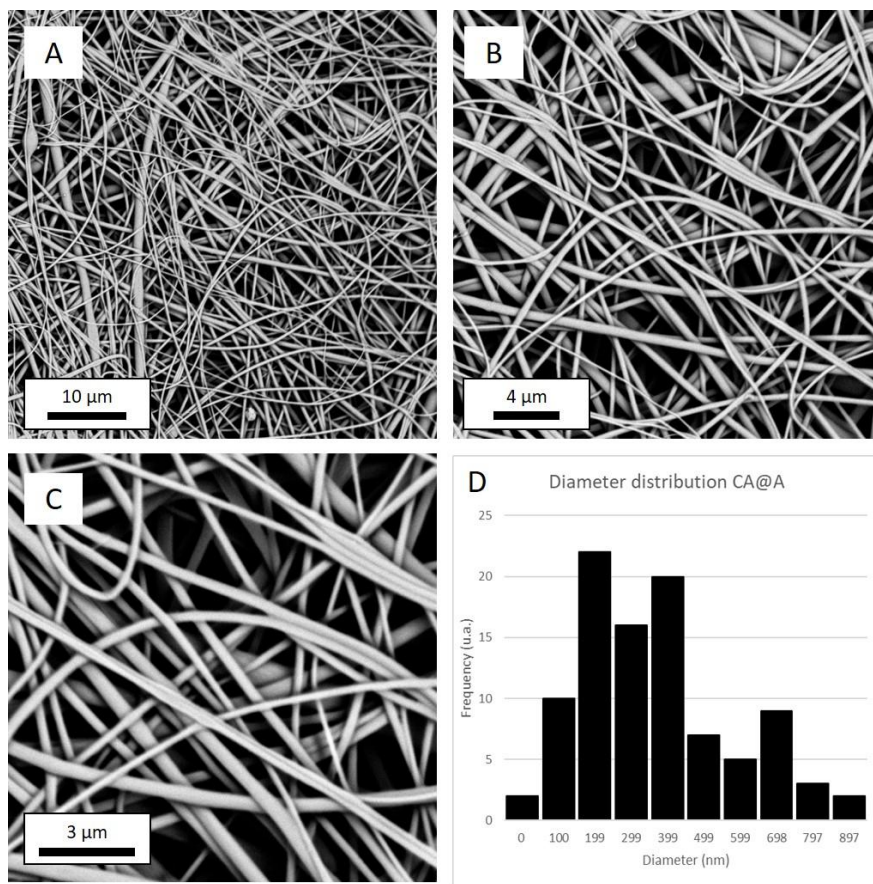


**Figure 4.** SEM images of cellulose acetate annatto (CA@A) nanofibers at different magnifications (A, B, C) and diameter distribution of CA@A nanofibers (D).

### 3.3 Thermal analysis of nanofibers

Figure 5 shows the TGA analysis for the CA and for the CA@A nanofibers.

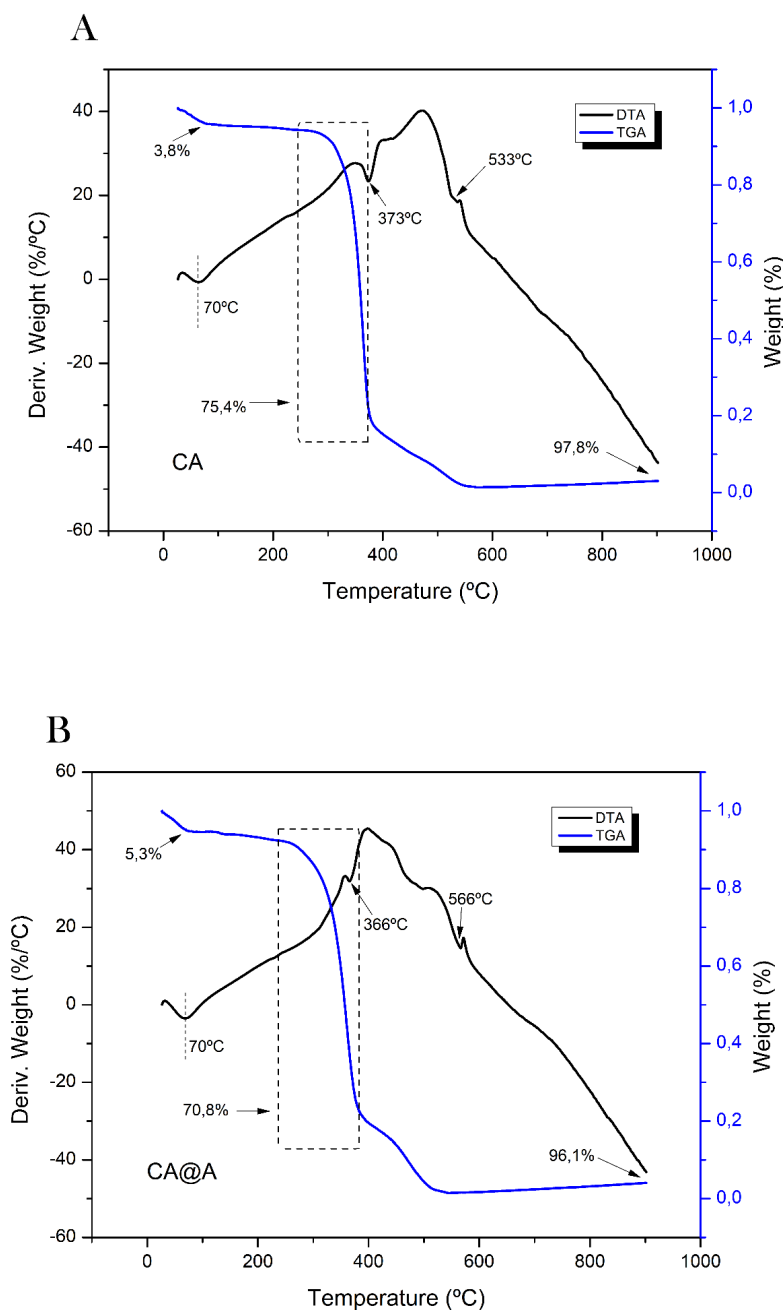


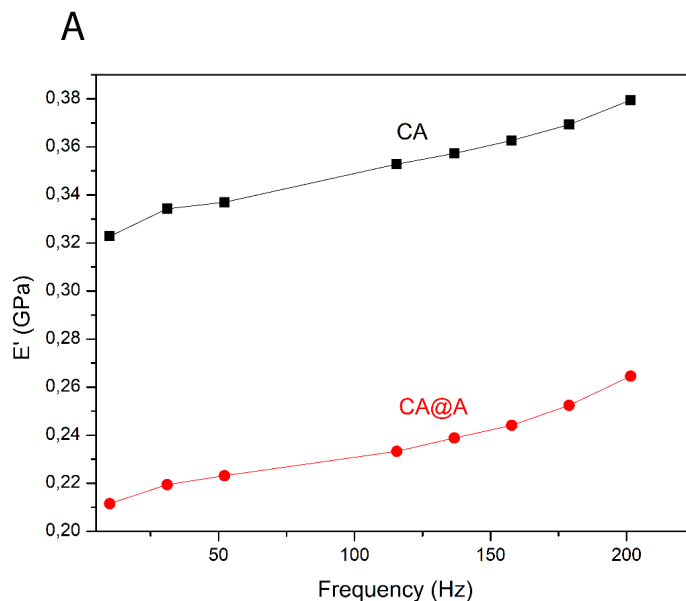
**Figure 5.** TGA and DTA curves for the cellulose acetate sample (CA) (A) and for the sample of cellulose acetate nanofibers with annatto extract (CA@A) (B).

For the neat sample, an initial weight loss (3.8%) was seen before reaching 100 °C; this could be the result of an endothermic water loss process [38] in which water is physically adsorbed between the CA molecular backbones. This initial weight loss is also ascribed to the remains of solvents between the nanofibers [39]. For the CA@A sample a higher weight loss (5.3%) before 100 °C was observed. The presence of annatto most likely increased the amount of water between the polymer molecules (hydrophilicity). A second weight loss

was observed between 245 °C and 373 °C for CA and between 237 °C and 383 °C for the CA@A samples. This second weight loss is attributed to thermal degradation of CA [26], deacetylation and pyrolytic decomposition of the polymer backbones (between 240 and 380 °C) [40]. The TGA results consequently suggest that CA was thermally stable during the preparation of the solution (25 °C) and electrospinning (25 °C), even when the annatto was present at 1% wt. Figure 5 (C) shows the weight loss curves for both the CA and CA@A samples; up to 275 °C a slight increase in thermal stability can be perceived for CA@A. The presence of annatto extract molecules may hamper the reactions involved in thermal degradation of CA. At 368 °C a crossover occurred, with inverted behavior above this temperature and the CA@A sample exhibiting a lower weight loss rate than the samples of neat CA. This phenomenon can be associated with the thermal degradation of bixin and norbixin molecules, which is reported to occur at 280–380 °C [41]. Another thermal event was observed around 533 °C for the CA sample and 566 °C for the CA@A sample, and can be attributed to carbonization of the remaining polymer [26]. The residual content at 900 °C was around 2.2% for the CA sample and 3.9% for CA@A.

### 3.4 Mechanical tests

Nano-DMA tests were performed to evaluate the influence of annatto on the viscoelastic behavior of the CA nanofibers. Figures 6 (A) and (B) show the storage moduli ( $E'$ ) and loss moduli ( $E''$ ), respectively.  $E'$  provides information about the energy stored elastically, while  $E''$  represents the viscous portion or the amount of energy dissipated in the sample.



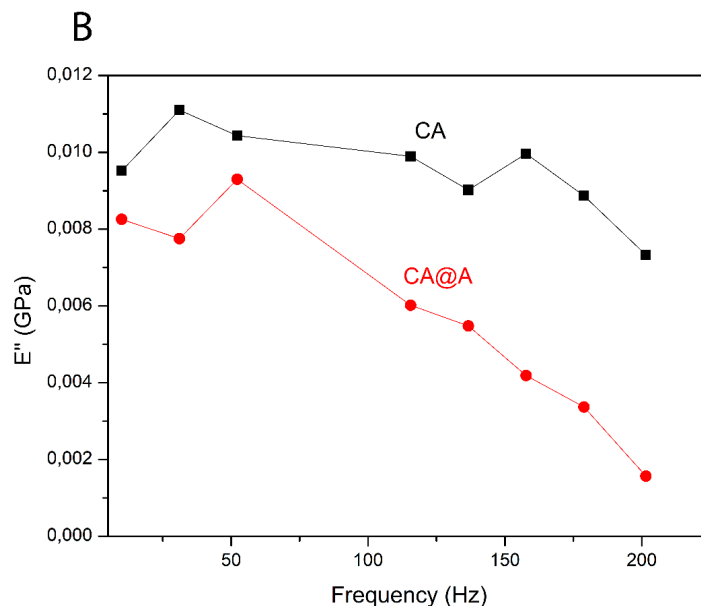


**Figure 6.** (A)  $E'(\omega)$  and (B)  $E''(\omega)$  curves for cellulose acetate (CA) and cellulose acetate nanofibers with annatto extract (CA@A) samples.

Adding annatto to CA causes reductions in both  $E'(\omega)$  and  $E''(\omega)$  throughout the broadband frequency range. When frequency tends to zero,  $E'$  is known to tend to  $E$  (the static modulus). For example, at 10 Hz  $E'(\omega)$  was 0.32277 GPa for the CA sample and 0.21148 GPa for the CA@A sample; in other words, adding annatto extract to CA reduced the storage modulus by 34.48%. The loss modulus at 10 Hz  $E''(\omega)$  was 0.00952 GPa for the CA sample and 0.00826 GPa for the CA@A sample, a reduction of 13.26%. This effect is usually seen when plasticizers are added to a polymer mass [42]. This suggests that annatto acted similar to a plasticizer, reducing interactions between the molecules and this leading to fewer entanglements and increased molecular motion, in turn generating greater deformation and a lower modulus.

### 3.5 Cell viability

C2C12 cell attachment in CA and CA@A scaffolds was assessed by counting cells after 24 hours of cell culture in GM (Figure 7A).

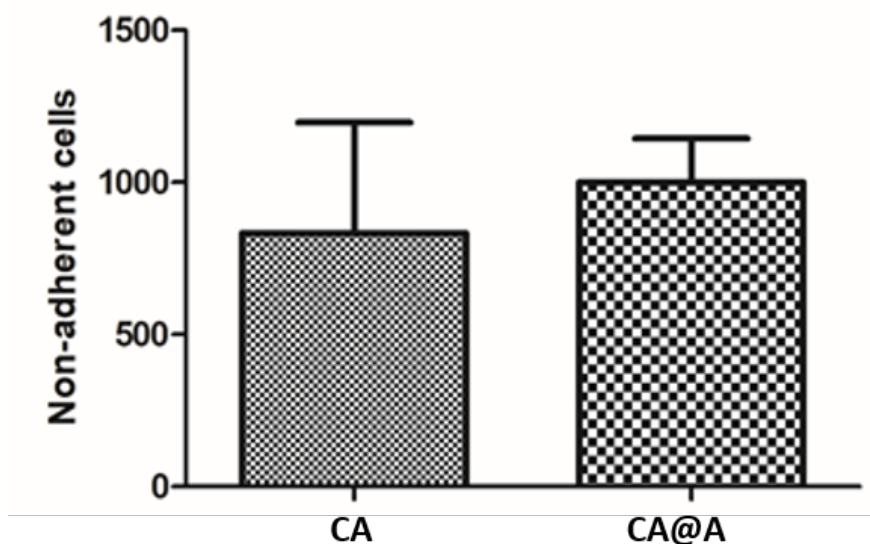


**Fig 7A.** C2C12 cell attachment to cellulose acetate (CA) and cellulose acetate nanofibers with annatto extract (CA@A) determined by cell counting after 24 h.

The results showed that fewer than 1,500 cells/well were unable to adhere to any substrate. The rates of adherent cells were approximately 97.5% and 98% for cells cultivated onto CA and CA@A scaffolds, respectively. No statistically significant difference was found between the cell number in the CA and CA@A nanofiber scaffolds, suggesting that both scaffolds permit significant cellular attachment.

The MTT assay was used to evaluate the viability and proliferation of C2C12 cells on CA and CA@A nanofibers.

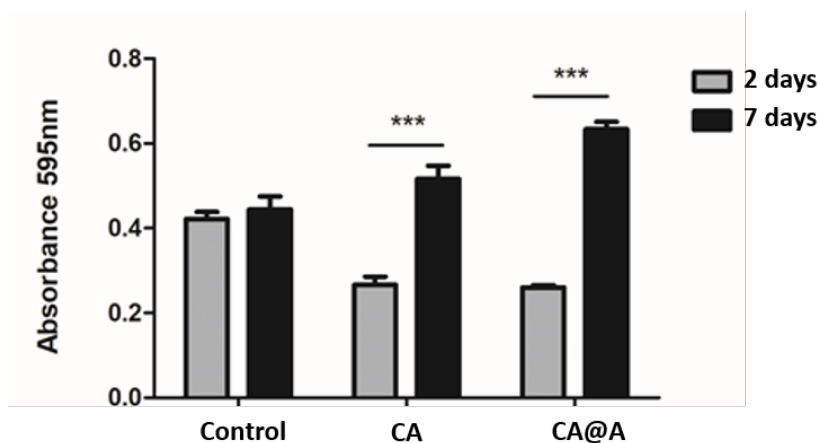


**Figure 7B.** MTT assay of C2C12 myoblast cells incubated onto well plate (control) and cellulose acetate (CA) and cellulose acetate nanofibers with annatto extract (CA@A) over 2 days and 7 days. \*\*\* $p < 0.05$  (Student's t-test)

Cells grown in a monolayer (control) were maintained under the same conditions and used for comparison. The MTT results (Figure 7B) obtained after 2 days of cell culture found lower cell viability in the scaffolds,

indicating that the monolayer control was more suitable than nanofiber scaffolds for cell attachment and proliferation during the initial days of culture.

After 7 days of culture, however, the cells in the monolayer reached growth arrest, while the viability rate for the cells cultivated onto the scaffolds increased. Growth arrest in the control may be regulated by cell-cell contact or contact inhibition [43]. This was not observed in cells cultivated onto nanofibers due to their large surface area, indicating that scaffolds are beneficial for longer-duration cell culture.

The viability of cells cultivated onto the CA@A nanofiber was also found to be higher than for those cultivated onto the CA nanofiber. Previous authors have shown annatto extract to be rich in antioxidant components that can improve cellular proliferation [44]. Furthermore, considering the more hydrophilic nature of cellulose acetate nanofiber with annatto (as demonstrated by the contact angle), this surface can also facilitate interactions between cells and matrices, leading to improved attachment and proliferation of C2C12 myoblasts [37]. These results suggest that CA@A nanofibers induce myoblast proliferation, which is essential for scaffolds utilized in cultivated meat expansion.

### 3.6 Cell morphology

The morphology of C2C12 cells in CA and CA@A nanofibers was analyzed via SEM after 2 and 7 days of cell culture.

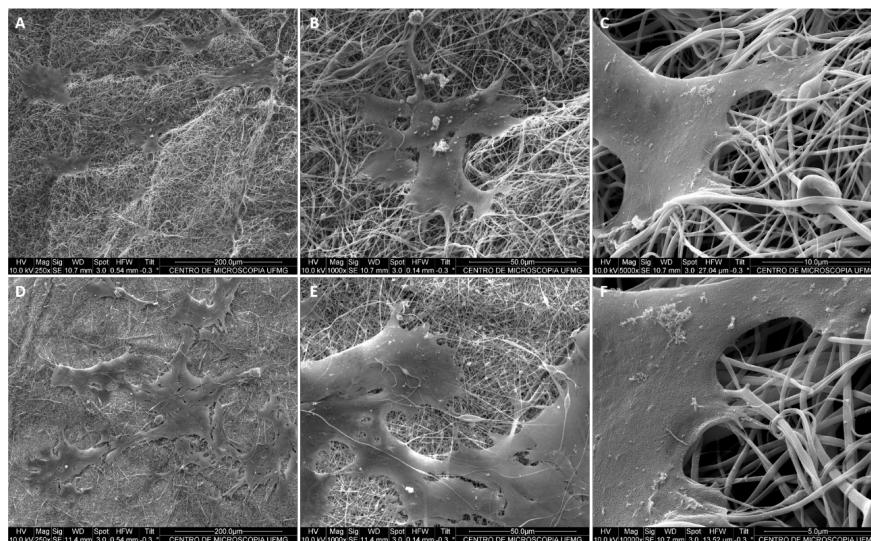


**Figure 8.** SEM images at different magnifications of C2C12 cells cultivated onto cellulose acetate nanofiber (A, B, C) and cellulose acetate nanofiber with annatto extract (D, E, F) after two days. Scale bars indicate (A,D) 200  $\mu\text{m}$ ; (B, E) 50  $\mu\text{m}$ ; (C, F) 5  $\mu\text{m}$ .

Figure 8 shows the morphology of C2C12 cells in nanofibers after 2 days of cell culture. The myoblasts can be seen in groups in both CA and CA@A nanofibers; more cell groups can be seen in the CA@A nanofiber (Figure 8 D). The magnified image reveals these interactions between neighboring cells, probably establishing the first cell-cell contacts (Figure 8 B, E). The cells were also well linked to the nanofibers (Figure 8 C, F) and had spindle-shaped morphology, similar to mononucleated myoblasts [45].

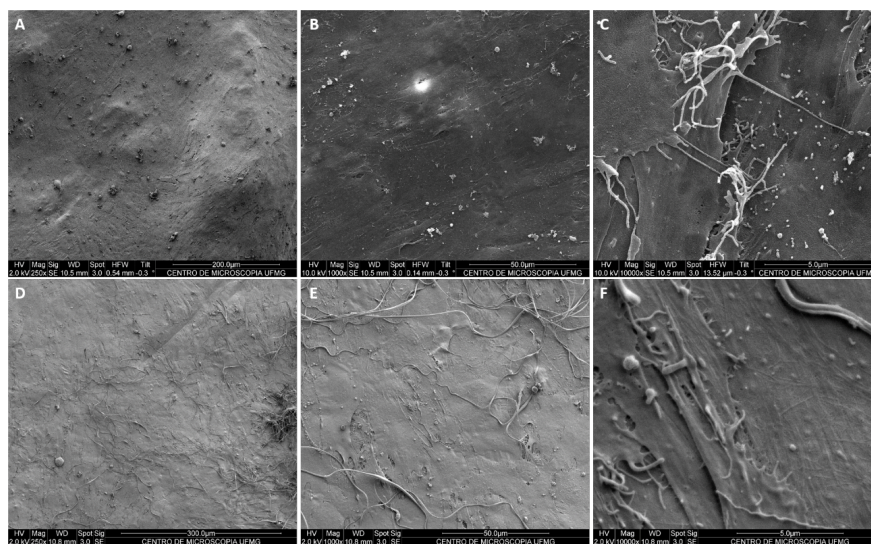


**Figure 9A.** SEM images at different magnifications of C2C12 cells cultivated onto cellulose acetate nanofiber (A, B, C) and cellulose acetate nanofiber with annatto extract (D, E, F) after seven days. Scale bars indicate (A) 200  $\mu\text{m}$ ; (D) 300  $\mu\text{m}$ ; (B, E) 50  $\mu\text{m}$ ; (C, F) 5  $\mu\text{m}$ .

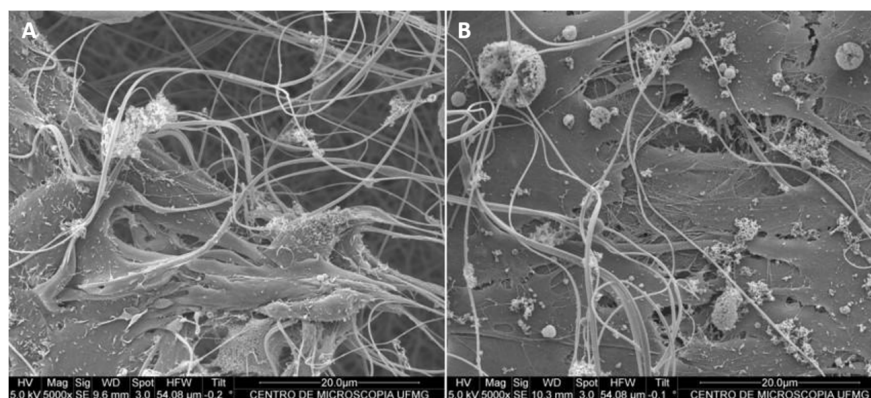


**Figure 9B.** SEM images showing cell infiltration of C2C12 cells cultivated onto cellulose acetate nanofiber (A) and cellulose acetate nanofiber with annatto extract (B) after seven days. Scale bars indicate 20  $\mu\text{m}$ .

Cell density increased exponentially after 7 days of culture to cover the surface of the nanofibers (Figure 9A). This corroborates the findings of the MTT test, in which viability for cells cultured onto the scaffolds was higher after 7 days of culture due to cell proliferation (Figure 7B). Almost all the cells stretched along the nanofibers and exhibited elongated morphology on the CA and CA@A nanofibers. According to Gurdon et al. (1996) [46], the community effect is a phenomenon involved in myogenesis in which muscle precursor cells must contact a sufficient number of like neighbors in order to undergo coordinated differentiation within developing tissue. Our findings indicate that cell-cell communication may play an important role in myogenic differentiation. Myoblasts covered by nanofibers were also present, suggesting cell migration through the pores of the scaffold (Figure 9B) and indicating that the porous nature of nanofiber scaffolds is ideal for myoblasts to infiltrate and may allow vascularization as well as multiple layers of skeletal muscle cells to form, both crucial processes for establishing a tissue-like construct [46].

### 3.7 Fluorescence microscopy of filamentous actin in C2C12 cells

The morphology of C2C12 cells cultivated on CA and CA@A scaffolds was also assessed using fluorescence images from staining F-actin, a component of the cell cytoskeleton (Figure 10).

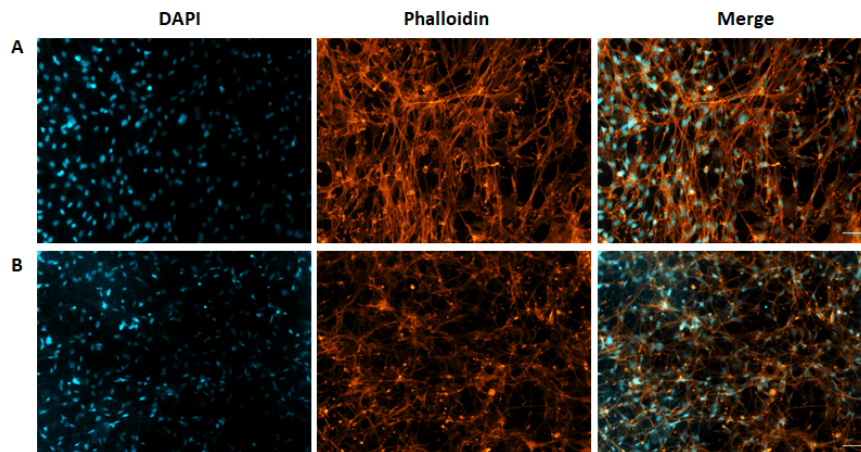


**Figure 10.** F-actin fluorescence staining in C2C12 cells cultivated for 7 days on cellulose acetate (A) and cellulose acetate nanofiber with annatto extract (B). Cell nuclei and F-actin were stained with DAPI (blue) and phalloidin (orange), respectively. Scale bar: 500  $\mu\text{m}$ .

To do so, cells were cultivated on the nanofibers for 7 days, since the actin cytoskeleton in this system is more easily resolved in higher density samples. C2C12 myoblasts can be found in a wide range of morphologies *in vitro* and progressively change shape during the fusion/differentiation process to become elongated and fusiform [47]. We found that the cells cultivated onto the CA nanofibers were aligned and elongated (Figure 10A), suggesting that they were beginning the differentiation process. The cells cultivated onto the CA@A nanofibers were thinner and elongated (Figure 10B), with random orientation of the actin cytoskeleton. This indicates that the shape of the cells growing in the CA nanofiber may be related to greater capacity for cell differentiation in this matrix, whereas myoblasts in the CA@A nanofibers may have a greater chance of proliferating before the differentiation process begins.

### 3.8 RT-qPCR

Expression levels of myogenic genes in C2C12 cells cultivated onto CA and CA@A scaffolds were determined using RT-qPCR to assess the progress of these cells during myogenic differentiation. C2C12 cells were cultivated onto both scaffolds in only GM, and *MyoD*, *Myf5*, and *MyoG* expression levels were evaluated after 7 and 14 days of culture.

We found upregulation of the expressions of *MyoD* (~4 fold change) and *MyoG* (~1.8 fold change) in the C2C12 cells cultivated onto CA scaffolds after 14 days compared to 7 days in culture; for *Myf5* in the same comparison, no effects were seen (Figure 11A). An entirely different gene expression pattern was seen when cells were cultivated onto CA@A scaffolds (Figure 11B): *MyoD* (~0.03 fold change) and *Myf5* (~0.100 fold change) were downregulated, while *MyoG* expression was upregulated after 14 days compared to 7 days in culture (Figure 11B). According to Chal et al. (2017) [48], *MyoD*, *Myf5*, and *MyoG* are directly linked to the cell differentiation stage in myogenesis, when cells assume a more elongated shape. *MyoD* and *Myf5* should be expressed first, since they are more related to the proliferation stage of these cells, while *MyoG* is related to the cell fusion stage and is necessary to form multinucleated myotubes [48]. Together, these results suggest that the CA scaffold favors cell proliferation and initiation of the first stages of skeletal muscle cell differentiation, while CA@A blocks the expression of the determination factors (*MyoD* and *Myf5*) and favors the terminal stages of cell differentiation.

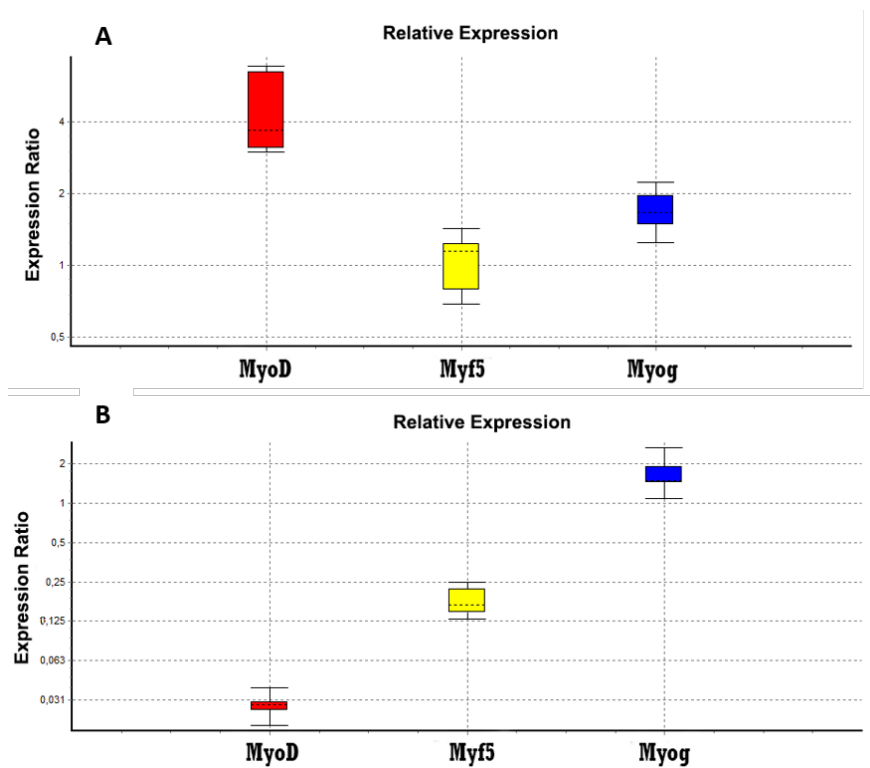


**Figure 11.** Relative expression levels of *MyoD*, *Myf5*, and *MyoG* in C2C12 cells cultivated in neat GM onto cellulose acetate nanofiber (A) and cellulose acetate nanofiber with annatto extract (B) after 14 days, compared to expression levels at 7 days.

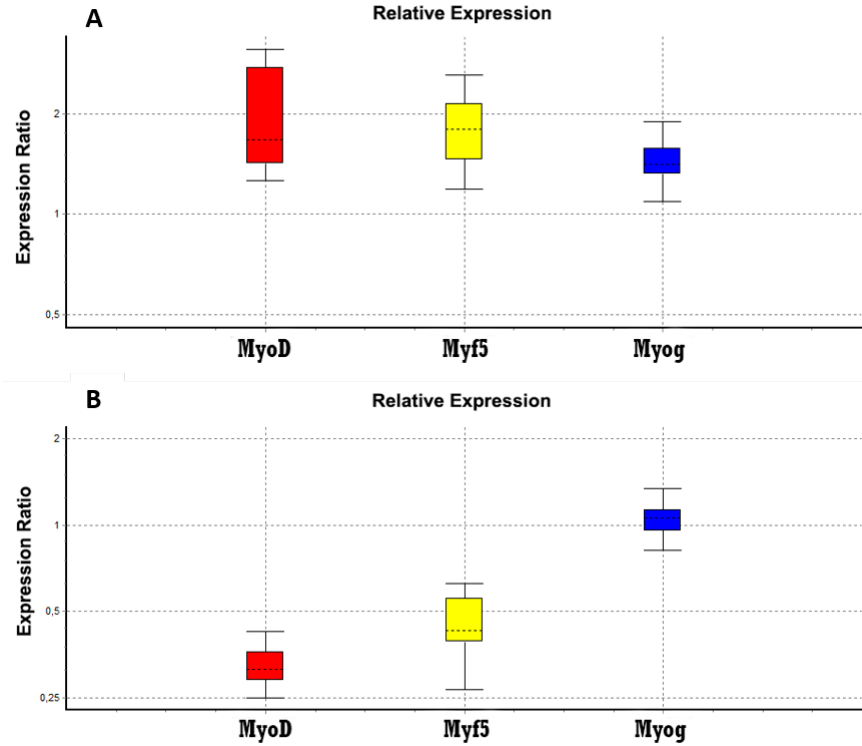


**Figure 12.** Relative expression levels of *MyoD*, *Myf5*, and *MyoG* in C2C12 cells cultured in GM for 7 days and in DM for an additional 7 days onto cellulose acetate nanofibers (A) and cellulose acetate nanofibers with annatto extract (B).

Minor differences in expression were observed when cells were cultivated onto CA and CA@A nanofibers for 7 days in GM, followed by 7 days in DM (Figure 12). Under these conditions, while the CA scaffold induced upregulation of expression of all the tested transcripts including *Myf5* (Figure 12A), CA@A's positive effect on *MyoG* expression was no longer visible but its negative effect on expression of the determination factors (*MyoD* and *Myf5*) remained (Figure 12B).

Therefore, these results corroborate the hypothesis that the CA scaffold with annatto in impairs the differentiation process, indicating that annatto extract does not synergize with the cell differentiation phenotype for C2C12 cells. However, the MTT assay results suggesting that annatto can improve C2C12 cell viability/proliferation indicate that this natural additive is useful when progenitor proliferation is required (for example, when establishing a construct for cultured meat production). A plausible hypothesis for the negative effect of annatto on myogenesis is that it can pair synergistically with other cell types, which is confirmed by research by Capella et al. (2016) [50], who found that annatto extract assisted in the process of healing open wounds when connective tissue was analyzed.

### 3.9 Long-term culture

Because of their large surface area relative to volume, nanofibrous substrates might offer more binding sites for initial cell attachment, in addition to longer periods of cell culture. However, few studies have investigated long-term maintenance of C2C12 cells cultivated onto scaffolds. In order to observe how C2C12 cells colonize both types of scaffolds, C2C12 was seeded onto the nanofibers and cultivated for 14, 21, and 28 days in GM for subsequent SEM analysis (Figure 13).

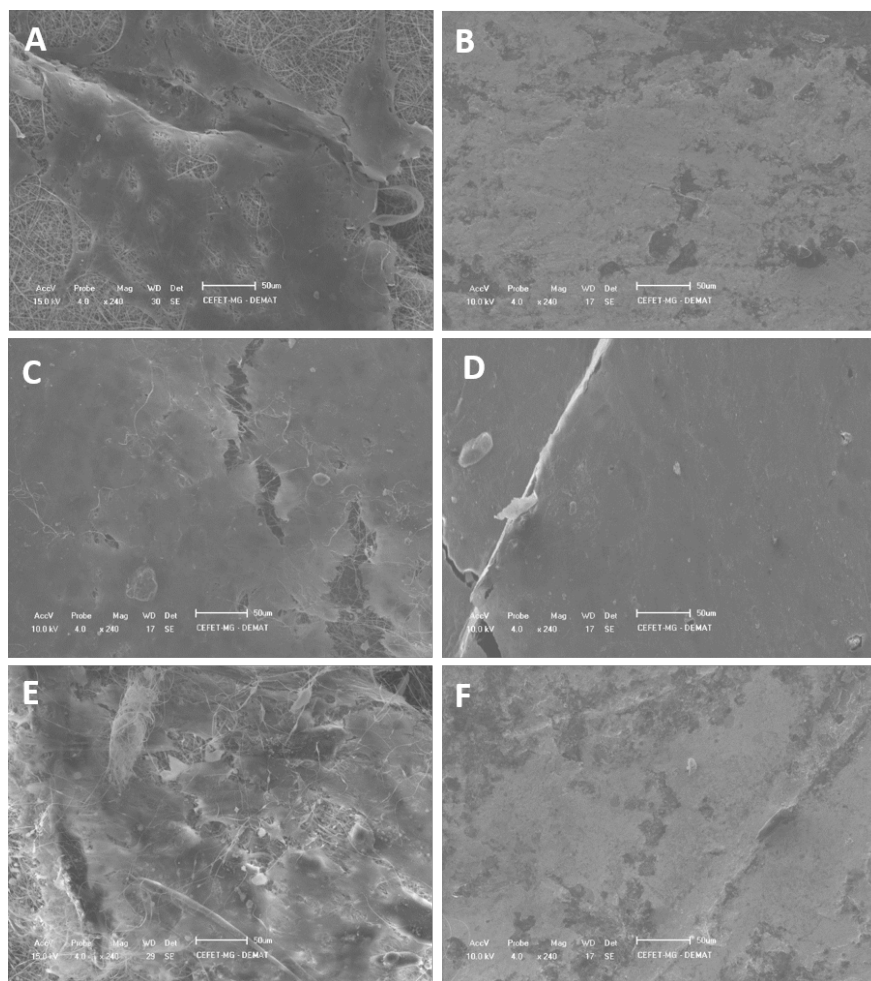


**Figure 13.** Scanning electron microscope images of C2C12 cells on cellulose acetate (CA) nanofibers (A, C, E) after 14, 21, and 28 days of cell culture, respectively, and cellulose acetate nanofibers with annatto extract (CA@A) (B, D, F) after 14, 21, and 28 days of cell culture, respectively. Scale bars indicate 50  $\mu\text{m}$ .

After 14 days of culture, cells completely covered the CA@A scaffold, while few cells were visible in the CA matrix (Figure 13). By 21 days, the CA scaffold was also entirely covered with cells. Figure 13 suggests that both the CA and CA@A nanofiber substrates can sustain long-term culture of C2C12 cells, up to 28 days. According to Choi et al. [49] and Post et al. [2], production of muscle cells in meat cultivation requires numerous muscle precursor cells, and consequently *in vitro* expansion of cells is a critical step for such applications. This present study suggests that annatto extract is useful in promoting rapid proliferation and coverage during the initial days of culture, providing sufficient quantities of muscle cells and thus permitting large-scale application for meat production. In addition, as already mentioned, annatto extract can be an important factor for the long-term preservation of the culture, avoiding unwanted contamination during the process. Future studies can be carried out to confirm the protective action of annatto extract as a meat preserver.

#### 4. Conclusion

Electrospinning cellulose acetate and cellulose acetate with annatto extract yielded nanofibers with porous structures and no specific alignment. Annatto extract provided a significant increase in the wetness of the nanofiber, boosting biocompatibility, but did not significantly affect the chemical or thermal stability of the

nanofibers. Mechanical analysis suggested that the annatto extract acts as a plasticizer between the polymer molecules.

*In vitro* testing confirmed that the porous nature of electrospun nanofibers permits cell migration and potential formation of multiple layers of muscle-like tissue, an essential property for meat cultivation. The nanofibers loaded with annatto extract were seen to induce myoblast proliferation in the MTT assay while delaying the onset of differentiation during myogenesis. Molecular analysis confirmed that CA nanofiber with annatto extract impaired the differentiation process, indicating that annatto extract does not synergize with the cell differentiation phenotype for C2C12 cells. In broad terms, these results suggest that cellulose acetate nanofiber loaded with annatto extract have potential for applications as a scaffold in the cultivated meat industry.

## Acknowledgments

The authors wish to thank the Coordination for the Improvement of Higher Education Personnel (CAPES, Brazil) for financial support, and Dr. Paul Zaslansky of the Department for Operative and Preventive Dentistry at Charité–Universitätsmedizin in Berlin, Germany for use of the Phenom SEM. Thanks to the Microscopy Center at the Federal University of Minas Gerais (<http://www.microscopia.ufmg.br>) for providing equipment and technical support for experiments involving electron microscopy. Thanks also to the Gamma Irradiation Laboratory installed at the Nuclear Technology Development Centre (CDTN), for the sterilization of the biomaterials.

**Data availability statement:** The data that support the findings of this study are available from the corresponding author upon reasonable request.

## References

- [1] Muhammad Sajid Arshad, Miral Javed, Muhammad Sohaib, Farhan Saeed, Ali Imran & Zaid Amjad | Fatih Yildiz (Reviewing Editor) (2017) Tissue engineering approaches to develop cultured meat from cells: A mini review, *Cogent Food & Agriculture*.
- [2] Post, M. J. (2012). Cultured meat from stem cells: Challenges and prospects. *Meat Science*, 92(3), 297–301.
- [3] Post, M.J., Levenberg, S., Kaplan, D.L. *et al.* Scientific, sustainability and regulatory challenges of cultured meat. *Nat Food* 1, 403–415 (2020).
- [4] Howard D, Buttery LD, Shakesheff KM, Roberts SJ. Tissue engineering: strategies, stem cells and scaffolds. *J Anat.* 2008;213(1):66-72. doi:10.1111/j.1469-7580.2008.00878.x
- [5] Xing H, Lee H, Luo L, Kyriakides TR. Extracellular matrix-derived biomaterials in engineering cell function. *Biotechnol Adv.* 2020;42:107421. doi:10.1016/j.biotechadv.2019.107421
- [6] Ahmad, Khurshid et al. “Extracellular Matrix and the Production of Cultured Meat.” *Foods (Basel, Switzerland)* vol. 10,12 3116. 15 Dec. 2021, doi:10.3390/foods10123116
- [7] Bomkamp, C.; Skaalure, S.C.; Fernando, G.F.; Ben-Arye, T.; Swartz, E.W.; Specht, E.A. Scaffolding Biomaterials for 3D Cultivated Meat: Prospects and Challenges. *Adv. Sci.* 2021, 9, 2102908.
- [8] BEN-ARYE, Tom; LEVENBERG, Shulamit. Tissue Engineering for Clean Meat Production. **Frontiers In Sustainable Food Systems**, [S.L.], v. 3, n. 0, p. 0-0, 18 jun. 2019. Frontiers Media SA. <http://dx.doi.org/10.3389/fsufs.2019.00046>.
- [9] Bentzinger, C. F.; Wang, Y. X.; Rudnicki, M. A.. Building Muscle: molecular regulation of myogenesis. *Cold Spring Harbor Perspectives In Biology*, v. 4, n. 2, 2012. Cold Spring Harbor Laboratory.
- [10] Djisalov M, Knežić T, Podunavac I, et al. Cultivating Multidisciplinary: Manufacturing and Sensing Challenges in Cultured Meat Production. *Biology (Basel)*. 2021;10(3):204. Published 2021 Mar 9. doi:10.3390/biology10030204
- [11] Hejazian L.B., Esmaeilzade B., Ghoroghi F.M., Moradi F., Hejazian M.B., Aslani A. The role of biodegradable engineered nanofiber scaffolds seeded with hair follicle stem cells for tissue engineering, Iran. *Biomed. J.* 2012;16:193–201
- [12] Baker BM, Mauck RL. The effect of nanofiber alignment on the maturation of engineered meniscus constructs. *Biomaterials*. 2007;28(11):1967-1977. doi:10.1016/j.biomaterials.2007.01.004
- [13] Hickey RJ, Pelling AE. Cellulose Biomaterials for Tissue Engineering. *Front Bioeng Biotechnol.* 2019;7:45. Published 2019 Mar 22. doi:10.3389/fbioe.2019.00045
- [14] Marino, A., Baronio, M., Buratti, U., Mele, E., & Ciofani, G. (2021). Porous Optically Transparent Cellulose Acetate Scaffolds for Biomimetic Blood-Brain Barrier *in vitro* Models. *Frontiers in bioengineering and biotechnology*, 9, 630063. <https://doi.org/10.3389/fbioe.2021.630063>
- [15] ELSAYED, Mardia T.; HASSAN,

Abeer A.; ABDELAAL, Said A.; TAHER, Mohamed M.; AHMED, Mohamed Khalaf; SHOUEIR, Kamel R.. Morphological, antibacterial, and cell attachment of cellulose acetate nanofibers containing modified hydroxyapatite for wound healing utilizations. **Journal Of Materials Research And Technology**, [S.L.], v. 9, n. 6, p. 13927-13936, nov. 2020. Elsevier BV. <http://dx.doi.org/10.1016/j.jmrt.2020.09.094>. [16] LIU, Haiqing; HSIEH, You-Lo. Ultrafine fibrous cellulose membranes from electrospinning of cellulose acetate. **Journal Of Polymer Science Part B: Polymer Physics**, [S.L.], v. 40, n. 18, p. 2119-2129, 8 ago. 2002. Wiley. <http://dx.doi.org/10.1002/polb.10261>. [17] N. Bifari, E., Bahadar Khan, S., A. Alamry, K., M. Asiri, A., & Akhtar, K. (2016). Cellulose Acetate Based Nanocomposites for Biomedical Applications: A Review. *Current Pharmaceutical Design*, 22(20), 3007–3019. [18] MITCHELL, Geoffrey R.; TOJEIRA, Ana. Role of Anisotropy in Tissue Engineering. **Procedia Engineering**, [S.L.], v. 59, p. 117-125, 2013. Elsevier BV. <http://dx.doi.org/10.1016/j.proeng.2013.05.100>. dos Santos, A. E. A., dos [19] MARZIO, Nicola di; EGLIN, David; SERRA, Tiziano; MORONI, Lorenzo. Bio-Fabrication: convergence of 3d bioprinting and nanobiomaterials in tissue engineering and regenerative medicine. **Frontiers In Bioengineering And Biotechnology**, [S.L.], v. 8, p. 0-3, 16 abr. 2020. Frontiers Media SA. <http://dx.doi.org/10.3389/fbioe.2020.00326>. [20] Hernández-Ochoa L, Aguirre-Prieto YB, Nevárez-Moorillón GV, Gutierrez-Mendez N, Salas-Muñoz E. Use of essential oils and extracts from spices in meat protection. *J Food Sci Technol*. 2014;51(5):957-963. doi:10.1007/s13197-011-0598-3 [21] Patra, Amlan Kumar. “An Overview of Antimicrobial Properties of Different Classes of Phytochemicals.” *Dietary Phytochemicals and Microbes* 1–32. 18 Feb. 2012, doi:10.1007/978-94-007-3926-0\_1 [22] Yousefi M, Khorshidian N and Hosseini H (2020) Potential Application of Essential Oils for Mitigation of *Listeria monocytogenes* in Meat and Poultry Products. *Front. Nutr.* 7:577287. doi: 10.3389/fnut.2020.577287 [23] Shahid-ul-Islam, Rather, L. J., & Mohammad, F. (2016). Phytochemistry, biological activities and potential of annatto in natural colorant production for industrial applications - A review. *Journal of Advanced Research*, 7(3), 499–514. [24] Rivera-Madrid, R., Aguilar-Espinosa, M., Cárdenas-Conejo, Y., Garza-Caligaris, L. E. Carotenoid Derivates in Achiote (*Bixa orellana*) Seeds: Synthesis and Health Promoting Properties. *Frontiers Plant Science*, 7, 21, 2016. [25] Cardarelli, C. R., Benassi, M. de T., & Mercadante, A. Z. (2008). Characterization of different annatto extracts based on antioxidant and colour properties. *LWT - Food Science and Technology*, 41(9), 1689–1693. [26] Santos, F. V., Freitas, K. M., Pimenta, L. P. S., de Oliveira Andrade, L., Marinho, T. A., de Avelar, G. F., da Silva, A. B., & Ferreira, R. V. (2021). Cellulose acetate nanofibers loaded with crude annatto extract: Preparation, characterization, and in vivo evaluation for potential wound healing applications. *Materials Science and Engineering C*, 118(November 2019), 111322. [27] Ning Xiang, John S.K. Yuen, Andrew J. Stout, Natalie R. Rubio, Ying Chen, David L. Kaplan, 3D porous scaffolds from wheat glutenin for cultured meat applications, *Biomaterials*, Volume 285, 2022, 121543, ISSN 0142-9612, <https://doi.org/10.1016/j.biomaterials.2022.121543>. [28] Pfaffl MW, Horgan GW, Dempfle L. Relative expression software tool (REST) for group-wise comparison and statistical analysis of relative expression results in real-time PCR. *Nucleic Acids Res*. 2002 [29] Giridhar, P. A Review on Annatto Dye Extraction, Analysis and Processing – A Food Technology Perspective. *Journal of Scientific Research and Reports*, 3, 327, 2014. [30] Calogero, G. Bartolotta, A., Di Marco G., Di Carlo A., Bonaccorso, F. Vegetable-based dye-sensitized solar cells. *Chemical Society Reviews*, 44, 3244, 2015. [31] Scotter, M. The chemistry and analysis of annatto food colouring: a review. *Food Additives and Contaminants*, 26, 1123, 2009. [32] Rahmalia, W., Fabre, J. F., Mouloungui, Z. Effects of Cyclohexane/Acetone Ratio on Bixin Extraction Yield by Accelerated Solvent Extraction Method. *Procedia Chemistry*, 14, 455, 2015. [33] Santos, L. F., Dias, V. M., Pilla, V., Andrade, A.A., Alves, L. P., Munin, E., Monteiro, V. S., Zilio. S. C. Spectroscopic and photothermal characterization of annatto: Applications in functional foods. *Dyes and Pigments*, 110, 72, 2010. [34] M.M. Meier, L.A. Kanis, V. Soldi, Characterization and drugpermeation profiles of microporous and dense cellulose acetate membranes: influence of plasticizer and pore forming agent, *Int. J. Pharm.* 278, 99–110, 2004. [35] Skornyakov, I.V., Komar, V.P. IR spectra and the structure of plasticized cellulose acetate films. *Journal of Applied Spectroscopy* 65, 911, 1998. [36] PINZÓN-GARCÍA, Ana Delia; CASSINI-VIEIRA, Puebla; RIBEIRO, Cyntia Cabral; JENSEN, Carlos Eduardo de Matos; BARCELOS, Luciola Silva; CORTES, Maria Esperanza; SINISTERRA, Ruben Dario. Efficient cutaneous wound healing using bixin-loaded PCL nanofibers in diabetic mice. *Journal Of Biomedical Materials Research Part B: Applied Biomaterials*, [S.L.], v. 105, n. 7, p. 1938-1949, 13 jun. 2016. Wiley. [37] Menzies, K. L., & Jones, L.

(2010). The impact of contact angle on the biocompatibility of biomaterials. *Optometry and Vision Science*, 87(6), 387–399. [38] Mandal, D. Chakrabarty. Studies on the mechanical, thermal, morphological and barrier properties of nanocomposites based on poly(vinyl alcohol) and nanocellulose from sugarcane bagasse. *Journal of Industrial and Engineering Chemistry*, 20, 462–473 (2014). [39] Santos, João Paulo Ferreira; da Silva, Aline Bruna ; Sundararaj, Uttandaraman ; Bretas, Rosario. Novel electrical conductive hybrid nanostructures based on PA 6/MWCNT COOH electrospun nanofibers and anchored MWCNT COOH. *Polymer Engineering and Science*, v. 55, p. n/a-n/a, 2015. [40] Candido, R. G., Godoy, G. G., & Gonçalves, A. (2017). Characterization and application of cellulose acetate synthesized from sugarcane bagasse. *Carbohydrate Polymers*, 167, 280–289. [41] SILVA, Marta C. D.; BOTELHO, J. R.; CONCEIÇÃO, Marta M.; LIRA, B. F.; COUTINHO, Monyque A.; DIAS, A. F.; SOUZA, A. G.; A. FILHO, P. F.. Thermogravimetric investigations on the thermal degradation of bixin, derived from the seeds of annatto (*Bixa orellana* L.). *Journal Of Thermal Analysis And Calorimetry*, [S.L.], v. 79, n. 2, p. 277 281, jan. 2005. Springer Science and Business Media LLC. [42] Vieira, M. G. A., Da Silva, M. A., Dos Santos, L. O., & Beppu, M. M. (2011). Natural-based plasticizers and biopolymer films: A review. *European Polymer Journal*, 47(3), 254–263. [43] Tanaka K, Sato K, Yoshida T, Fukuda T, Hanamura K, Kojima N, Shirao T, Yanagawa T, Watanabe H. Evidence for cell density affecting C2C12 myogenesis: possible regulation of myogenesis by cell-cell communication. *Muscle Nerve*. 2011 [44] Bruno Oliveira Silva Duran, Guilherme Alcarás Góes, Bruna Tereza ThomaziniZanella, Paula Paccielli Freire , Jessica Silvino Valente, Rondinelle Artur Simões Salomão, Ana Fernandes, Edson Assunção Mareco, Robson Francisco Carvalho & Maeli Dal-Pai-Silva. Ascorbic acid stimulates the in vitro myoblast proliferation and migration of pacu (*Piaractus mesopotamicus*). *Scientific Reports* (2019) 9:2229 [45] SNOW, Mikel H. Myogenic cell formation in regenerating rat skeletal muscle injured by mincing I. A fine structural study. *The Anatomical Record*, [S.L.], v. 188, n. 2, p. 181-199, jun. 1977. [46] GURDON, J.B.; LEMAIRE, P.; KATO, K. Community effects and related phenomena in development. *Cell*, [S.L.], v. 75, n. 5, p. 831-834, dez. 1993. [47] Bruyère, C., Versaavel, M., Mohammed, D. *et al.* Actomyosin contractility scales with myoblast elongation and enhances differentiation through YAP nuclear export. *Sci Rep* 9,15565 (2019). [48] Chal, J., & Pourquié, O. (2017). Making muscle: Skeletal myogenesis in vivo and in vitro. *Development (Cambridge)*, 144(12), 2104–2122. [49] CHOI, Kwang-Hwan; YOON, Ji Won; KIM, Minsu; LEE, Hyun Jung; JEONG, Jinsol; RYU, Minkyung; JO, Cheorun; LEE, Chang-Kyu. Muscle stem cell isolation and in vitro culture for meat production: a methodological review. *Comprehensive Reviews In Food Science And Food Safety*, [S.L.], v. 20, n. 1, p. 429-457, 6 nov. 2020. Wiley. [50] Capella, S. O., Tillmann, M. T., Felix, A. O. C., Fontoura, E. G., Fernandes, C. G., Freitag, R. A., Santos, M. A. Z., Felix, S. R., & Nobre, M. O. (2016). Potencial cicatricial da *Bixa orellana* L. em feridas cutâneas: Estudo em modelo experimental. *Arquivo Brasileiro de Medicina Veterinaria e Zootecnia*, 68(1), 104–112.